Density Functional Study of Excited Charge Transfer State Formation in 4-(*N*,*N*-Dimethylamino)benzonitrile

Andreas B. J. Parusel*,† and Gottfried Köhler

Institute for Theoretical Chemistry and Radiation Chemistry, University of Vienna, Althanstrasse 14, 1090 Vienna, Austria

Stefan Grimme‡

Institute for Physical Chemistry and Theoretical Chemistry, University of Bonn, Wegelerstrasse 12, 53115 Bonn, Germany

Received: November 5, 1997; In Final Form: February 18, 1998

The excited singlet states of 4-(*N*,*N*-dimethylamino)benzonitrile (DMABN), 4-*N*,*N*-dimethylaminobenzaldehyd (DMABA), and methyl 4-*N*,*N*-dimethylaminobenzoate (DMABME) are studied by a combination of density functional theory and configuration interaction approaches (DFT/SCI). DMABN is investigated in more detail as the best known model system showing dual fluorescence in polar solvents. Because the origin of the second red-shifted fluorescence is still not settled definitely, we consider three commonly discussed geometric relaxation pathways which generate low lying intramolecular charge transfer states (TICT, WICT, and RICT). In general, the results of the DFT/SCI calculations for excitation energies, oscillator strengths, and dipole moments compare favorably with either experimental results or data from very elaborate theoretical CASPT2 calculations. For DMABN we find a global minimum structure in the first excited state with a twisted (60°) but not pyramidalized dimethylamino group. The barrier for TICT state formation from the lowest $1B_2$ state is computed to be 2.3 kcal/mol. The calculated vertical fluorescence band energy of 3.4 eV is in good agreement with experimental data (3.2 eV). The rehybridization of the cyano group according to the RICT model leads also to an excited-state minimum with strong charge-transfer character. However, this RICT state lies higher in energy than the TICT state and is furthermore associated with a large barrier (17.6 kcal/mol). The results of the DFT/SCI calculations for the keto derivatives DMABA and DMABME reveal, in agreement with experiment, quite a small splitting between the lowest L_b and L_a states (≈0.15 eV).

1. Introduction

Interest in the dual fluorescence phenomenon has attracted increasing attention since its discovery by Lippert et al.[1] 35 years ago. Lippert ascertained an anormal emission (^1L_a according to Platt's notation[2]), red-shifted from the normal ^1L_b fluorescence for 4-(*N*,*N*-dimethylamino)benzonitrile (DMABN, see Figure 1) in polar solvents. This low-energy emission band is found in several other electron donor−acceptor compounds as well. All molecules are of a general donor−acceptor pattern with both subunits connected by a single bond.[3−5] Numerous compounds emitting dual fluorescence are known by now, but the origin of this unusual property is not completely understood at present, and various mechanisms have been suggested since then. Lippert et al.[1] primarily assigned the two distinct emission bands to two different low-lying excited singlet states which invert in polar solvents. Several proposals were made in the next decades, such as excimer formation by McGlynn et al.,[6] excited-state proton transfer by Kosower et al.,[7] and exciplex formation by Chandross[8] and Visser et al.[9] Intersystem crossing is generally the most important deactivation channel of DMABN.[10] The sum of fluorescence and intersystem crossing quantum yield Φ is near unity, and further deactivation processes can be excluded in nonpolar and gas-phase conditions.

Nowadays, the TICT (twisted intramolecular charge transfer) model of Grabowski et al.[11,12] is widely accepted as an explanation of the dual fluorescence phenomenon. According to this model, the ^1L_b emission arises from a planar first excited state of DMABN. The anormal fluorescence is attributed to a highly polar state that is formed by twisting of the dimethylamino donor group perpendicular to the benzene plane (see Figure 2) accompanied by an intramolecular charge transfer (CT) from the donor (dimethylamino group) to the acceptor moiety (benzonitrile group). This rotation leads to an energetically stabilized excited-state conformation, which is depopulated to the electronic ground state by fluorescence emission. Several experimental results seem to corroborate this hypothesis: derivatives of DMABN with the amino group forced to planarity by incorporation into five- and six-membered rings exhibit only the normal fluorescence band.[13−16] Systems with sterical hindrance to planarity such as 6-cyanobenzquinuclidine (CBQ)[12,17] or *N*,*N*-3,5-tetramethyl-4-aminobenzonitrile (TMABN)[18] are

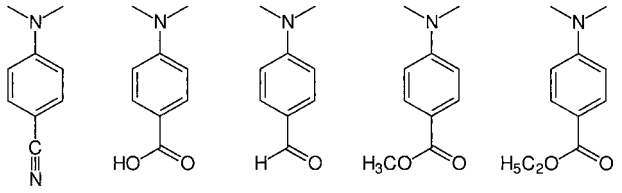

Figure 1. Structures of DMABN and its keto derivatives.

† Fax: +43 1 31336 790. E-mail: andreas@majestix.msp.univie.ac.at.
‡ Fax: +49 228 73 9066. E-mail: grimme@rs3b.thch.uni-bonn.de.

S1089-5639(98)00086-3 CCC: $15.00
Published on Web 07/10/1998

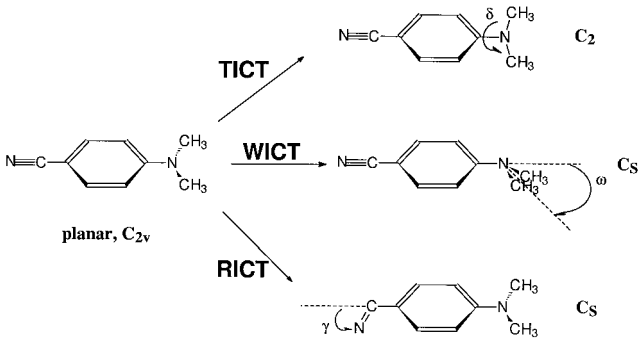

Figure 2. Models of the DMABN relaxation modes according to the TICT (twisting angle δ), WICT (wagging angle ω), and RICT (bending angle γ) approaches.

pretwisted in the electronic ground state and yield only one L_a state emission.

According to the TICT model, decoupling of the donor and acceptor orbitals by twisting the dimethylamino subunit is the driving force for the formation of a low lying excited CT state in DMABN. Zachariasse et al.[19−23] postulated that the nitrogen lone pair can also be decoupled from the benzonitrile π system by pyramidalization (wagging) of the dimethylamino group (rehybridization from sp^2 to sp^3 at the nitrogen atom). A small energy gap and a solvent-induced vibronic coupling between the first and second excited states should increase the localization of the positive charge on the donor and negative charge on the acceptor subunit, respectively. Gorse and Pesquer[24] proposed that large wagging angles decouple the donor from the acceptor orbitals as well, generating an intramolecular CT state with an increased dipole moment (WICT, wagged intramolecular charge transfer).[24]

Numerous theoretical studies on DMABN using both semiempirical[12,24−37] and ab initio[38−44] methods have been carried out. Most of them confirm the validity of the TICT model, although many of them are based on very approximate methods. However, also the correlated ab initio CASPT2 calculations by Serrano-Andrés et al.[42] yield the same conclusion.

Recently, Sobolewski and Domcke[43,44] discussed a highly polar excited state with an in-plane bent cyano group (RICT model: rehybridization by intramolecular charge transfer). Employing the CASPT2 method, a local minimum on the potential energy surface of the first excited state with an sp^2 hybridized carbon atom was found (the bending angle C4−C7−N8 is calculated to be about 120°; for the labeling see Figure 3).

4-*N*,*N*-Dimethylaminobenzoic acid (DMABAc),[45] 4-*N*,*N*-dimethylaminobenzaldehyd (DMABA),[46] and various esters (see Figure 1) of DMABAc[47−52] have been known to show anomalous fluorescence properties as well. In the gas phase the ^1L_a state for methyl and ethyl 4-*N*,*N*-dimethylaminobenzoate (DMABME and DMABEE, respectively) is located approximately at the same energy as the ^1L_b state. For DMABA this ordering is reversed in the nonpolar hexane solvent. The ^1L_b and ^1L_a states seem to lie energetically very close, and a strong state mixing is deduced from fluorescence experiments.[48,49,51] This observation (substituent effect) is an excellent test for any theoretical method to prove its reliability, and thus, both DMABA and DMABME have been included in our study.

Accurate methods for the description of excited states, such as CASPT2[53] and multireference configuration interaction methods (MR[SD]-CI),[54] are limited to relatively small systems with high symmetry. Recently, one of us developed a combination of density functional theory (DFT; for a survey of ground-

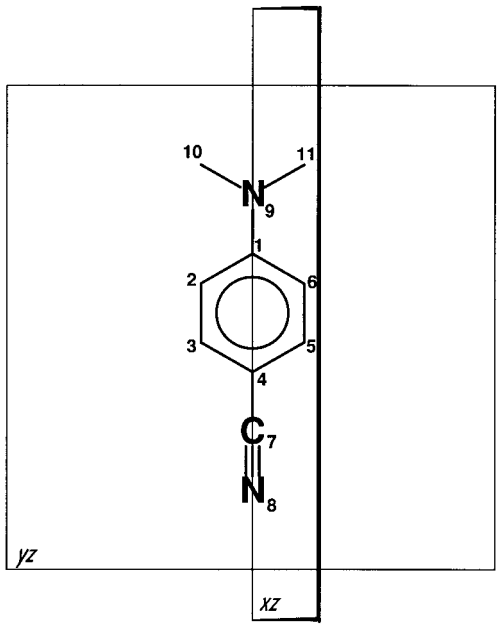

Figure 3. Enumeration and molecular planes defining the symmetry of DMABN.

state DFT see, for example, ref 55) with the configuration interaction method including only single excitations (DFT/SCI)[56] for a description of excited states. The inclusion of dynamical electron correlation effects in the DFT/SCI method gives more reliable results compared to the standard Hartree−Fock/SCI (also termed CIS) approach. The DFT/SCI method has been satisfactorily tested in the interpretation of vis/UV and CD spectra of a wide range of molecules.[56−60] On the average the errors for vertical excitation energies do not exceed 0.2−0.3 eV and also transition moments are described very accurately. Although the DFT/SCI approach is restricted to single excitations, it implicitly accounts for higher excitation classes (i.e., doubles and triples) and thus for the most important dynamical electron correlation effects. This is of particular importance in aromatic hydrocarbons (e.g., as in DMABN) where the ab initio CIS approach often gives the wrong ordering of excited states of different character (e.g., L_a vs L_b, cf. section 4). Although the method is semiempirical in nature (there are four parameters which depend only on the exchange−correlation functional used), it has a deep theoretical foundation because it represents an approximate version of time-dependent density functional theory (see for example refs 61, 62).

In the present work we use DMABN as a test case for the performance of the DFT/SCI method to describe the excited singlet states of CT systems. Although the TICT phenomenon is strongly related to solvation, the theoretical results corresponding to the gas phase can be compared with ab initio CASPT2 data or experimental results obtained in nonpolar solvents. To check the validity of several hypotheses, the twisting motion of the dimethylamino group (according to the TICT model) is taken into account as well as the wagging mode of the amino group (WICT model) and the in-plane bending angle of the cyano group (RICT model). Evolution of excitation energies, oscillator strengths, and dipole moments along these reaction coordinates and a characterization of the excited singlet states is presented. Additionally, the influence of wagged conformations on the twisting coordinate is analyzed. It will be shown that the DFT/SCI method produces results that have at least CASPT2 quality at very little computational effort, which makes it well suited for future studies on larger CT systems. To the best of our knowledge, reliable theoretical investigations

TABLE 1: Low Lying Excited Singlet States of Planar DMABN (C_{2v}) at the DFT/SCI(VDZP) Level with Vertical Excitation Energies ΔE (in eV), Oscillator Strenghs f, Dipole Moments μ (in D), and Weights of the Dominating One-Electron Configurations in the CI Wave Functions

	state	ΔE	f [a]	μ	energy[b]	one-electron transition	
S_1	$1B_2$	4.05	0.027	11.5	−0.079 13	HOMO → LUMO+1	83%
						HOMO-1 → LUMO	15%
S_2	$2A_1$	4.56	0.658	16.0	−0.060 37	HOMO → LUMO	90%
S_3	$2B_2$	5.70	0.118	14.2	−0.018 32	HOMO-1 → LUMO	62%
						HOMO-2 → LUMO+1	24%
S_4	$1A_2$	6.27	0.000	18.1	+0.002 47	HOMO → LUMO+2	80%
S_5	$3A_1$	6.31	0.016	5.9	+0.003 90	HOMO-2 → LUMO	85%
S_6	$4A_1$	6.71	0.836	8.91	+0.018 65	HOMO-2 → LUMO+1	76%
						HOMO-4 → LUMO	10%

[a] Oscillator strength obtained from the lengths formalism. [b] Total energy +458 au.

for the first excited states of DMABA and DMABME are presented here for the first time.

2. Methods and Computational Details

For an enumeration and definition of the coordinate system used for DMABN see Figure 3. The molecule is placed in the *yz* plane with the long molecular axis parallel to *z*. The twisting angle is defined as the dihedral angle of the dimethylamino group with the benzene moiety (δ(C10−N9−C1−C2)). Gradual rotation by 10° from 0° to 90° is considered. For the planar ($\delta = 0°$) and perpendicular ($\delta = 90°$) conformations C_{2v} symmetry is assumed, whereas the other computations are carried out employing C_2 symmetry. For wagging angles ω (for a definition see Figure 2) values of 0°, 10°, 20°, 30°, 40°, and 50° are considered. The RICT coordinate, defined by the bending angle γ(C4−C7−N8), is computed in steps of 10° from 180° (sp hybridization) to 120° ($\approx sp^2$ hybridization), with an additional computation at 110°. Inspection of the results of Sobolewski and Domcke[44] shows that the CN bond length increases along the bending coordinate. This stretch motion is also in accordance with the time-resolved infrared spectroscopy studies of Hashimoto and Hamaguchi.[63] Thus we decided to increase this distance linearly from 1.14 Å (at $\gamma = 180°$) to 1.34 Å at 110°. C_s symmetry is used in these calculations, with DMABN placed in the *yz* plane.

All DFT calculations have been carried out with the TURBOMOLE suite of programs.[64,65] We have tested various methods (AM1, HF-SCF, DFT) for the optimization of DMABN in its ground state, but it turned out the DFT approach gives the best results for the excitation energies and also the lowest total excited-state energies. Throughout this work we employ the nonlocal exchange correlation functional of Becke and Lee, Yang, and Parr in its hybrid form, i.e., including some portion of exact HF exchange (B3LYP).[66,67] If not stated otherwise, a valence double-ζ basis set including polarization functions on all atoms (C, N, O; [3s2p1d]; H: 2s1p, VDZP)[68] is used. All reaction coordinate calculations were performed with the DFT-B3LYP/VDZP optimized ground-state geometry of DMABN, i.e., only the coordinates δ, ω, and γ/r_{CN} are varied, while the other geometric parameters are kept fixed at their optimized ground-state values. In the SCI calculations the 1s electrons are kept frozen, while all valence and virtual orbitals are used to construct the spin-adapted configuration-state functions (4620 in C_1 symmetry). Results obtained with smaller basis sets are of interest to forthcoming calculations on larger molecular systems. They are subject to a detailed investigation discussed in section 3.1. For DMABA and DMABME the DFT-B3LYP/VDZP optimized ground-state geometry with C_s symmetry was employed in all calculations.

3. Results

3.1. Ground-State Properties and Vertical Excited States of DMABN. The B3LYP/VDZP optimized ground-state geometry of DMABN is found to be planar, possessing C_{2v} symmetry. The experimentally known pyramidalization[69,70] cannot be corroborated with the VDZP basis set. The slight pyramidalization angle ω found theoretically (21.2° by CAS-SCF[42]) and deduced from experiments (12°[69] and 15°,[70] respectively) is known to be separated only by a few kcal/mol from a planar transition state of C_{2v} symmetry. With a large TZ2P basis set (see below) we correctly obtain at the B3LYP level a nonplanar structure with $\omega = 14.2°$ and an inversion barrier of approximately 0.1 kcal/mol. This negligibly small barrier corresponds to the experimentally known free inversion motion of DMABN. The effect of a 20° pyramidalization on the TICT coordinate is investigated in section 3.2.

The calculated ground-state dipole moment of 8.0 D is in reasonable agreement with experimental data, ranging from 5 to 7 D.,[11,12,19,71−75] The first six excited singlet states of DMABN are characterized in Table 1 along with their excitation energies, oscillator strengths, and dipole moments. The first excited state with B_2 symmetry is dominated by the one-electron excitation HOMO → LUMO+1, with a small contribution from the HOMO-1 → LUMO promotion and a partial CT from the dimethylamino to the benzene subunit. The $2A_1$ state with almost exclusive HOMO → LUMO character has a large dipole moment (16 D) and a large oscillator strength and is observed as the most intense band in the absorption spectrum (cf. section 4). The second and third excited states are of partial CT character. The third excited state with a slightly smaller dipole moment (14.2 D) is characterized by a $\pi_{benzene} \rightarrow \pi^*_{benzonitrile}$ excitation. The S_4 state, with a dipole moment of 18.1 D, is characterized by a CT from the dimethylanilino to an in-plane π^*_x orbital localized at the cyano group. The fifth and sixth excited states $3A_1$ and $4A_1$ are of locally excited (LE) character, mainly described by $\pi\pi^*$ excitations within the benzene group. All higher excited states as computed by DFT/SCI are in good agreement with experimental data derived from electron energy loss spectroscopy.[76]

DMABN is known as the smallest compound emitting dual fluorescence. Several other larger molecules that show this unusual spectroscopic property are of interest as a fluorescence probe in biological environments[3] or as chromophores with high nonlinear optical properties.[77] These large molecules can be investigated by the DFT/SCI method as well, but the VDZP basis set will lead to huge computation times. Thus we investigated the basis set dependence for some properties of the first two excited states of DMABN. The smallest basis is the VDZ set where all polarization functions from the VDZP set have been discarded. With the VDZ+d basis the effect of

TABLE 2: Effect of Different Basis Sets on the Vertical Excitation Energies ΔE (in eV), Oscillator Strenghs f, and Dipole Moments μ (in D) for the Three Lowest Singlet States of Planar DMABN

		VDZ	VDZ+d	VDZP	TZ2P[a]	expt[b]
number of AOs		119	174	204	335	
CPU time[c]		1.0	3.8	5.2	38.5	
ground state	μ	8.08	7.98	8.00	7.99	5−7
$1B_2$	ΔE	4.13	4.07	4.05	4.02	4.0
	μ	11.82	11.42	11.49	11.39	8−11
	f	0.029	0.026	0.027	0.030	0.04
$2A_1$	ΔE	4.65	4.57	4.56	4.52	4.4
	μ	17.16	15.92	15.98	15.64	11−14
	f	0.700	0.663	0.658	0.663	0.33

[a] Exponents of the polarization functions: d(C) = 1.1, 0.3; d(N) = 1.6, 0.5; p(H) = 0.8. [b] Refs 11, 12, 19, 71−75, 79. [c] Relative to the VDZ calculation, which took 6 min on one processor of a HP/CONVEX PA8000 computer.

adding d-functions to the non-hydrogen atoms is evaluated. The results obtained with a triple-ζ valence basis set with two polarization functions at the C and N atoms (C, N: 6s3p2d, H: 3s1p, TZ2P[78]) can be considered to be near the basis set limit.

It is obvious from inspection of Table 2 that the results depend very little on the quality of the basis set employed. No change in succession of the excited states is found. The excitation energies decrease slightly with increasing quality of the basis set. Even the VDZ basis yields excitation energies only 0.2 eV too high in comparison to experiment. The best basis set used in our comparative study (TZ2P) reproduces the experimental results very accurately, i.e., within the experimental error limits. The dipole moments and oscillator strengths are also not subject to any significant changes. The VDZ+d and even the VDZ basis set can therefore be used without reservation for larger molecules where the basis set requirements are known to be of less importance. The results in Table 2 also underline the efficiency of the VDZP basis set, which is used for all following calculations. The CPU time is less than twice as long as for the VDZ+d set, but we notice an improvement of the results. In contrast, the results determined with the TZ2P basis are only slighty better compared to those at the VDZP level, but the CPU time increases by a factor of 8.

3.2. Potential Curves for the Twisting Mode. The results obtained for excitation energies and dipole moments for nonwagged DMABN along the twisting coordinate δ, in steps of 10°, are presented in Figure 4. The free electron pair character of the HOMO increases along the reaction coordinate, and for $\delta = 90°$ the HOMO represents a pure free amino electron pair. Thus, the CT character for all transitions that involve the highest occupied orbital increases significantly. The total energy of the first excited state of B symmetry increases upon rotation and is, at $\delta = 90°$, quite close to the second excited state of B symmetry (S_3 at $\delta = 0°$), which is stabilized along the path. These two B states show a different behavior in the evolution of dipole moment. The partial CT character of the first B state, which is mainly described by the HOMO → LUMO+1 transition, increases from 11.5 to 18.5 D. On the contrary, the dipole moment of the 2B state decreases monotonically from 14.2 to 5.9 D and becomes of locally excited character at $\delta = 90°$. A different dipole moment evolution is found for the 2A state, which rises from 11.5 to 19.3 D upon rotation from 0 to 90°. Similarly, the oscillator strength decreases from 0.66 to 0.00 at 90°, where the transition is symmetry forbidden ($A_1 \rightarrow A_2$). This strong dependence of the electric dipole transition moment values on the twisting angle is of particular importance for the TICT fluorescence emission

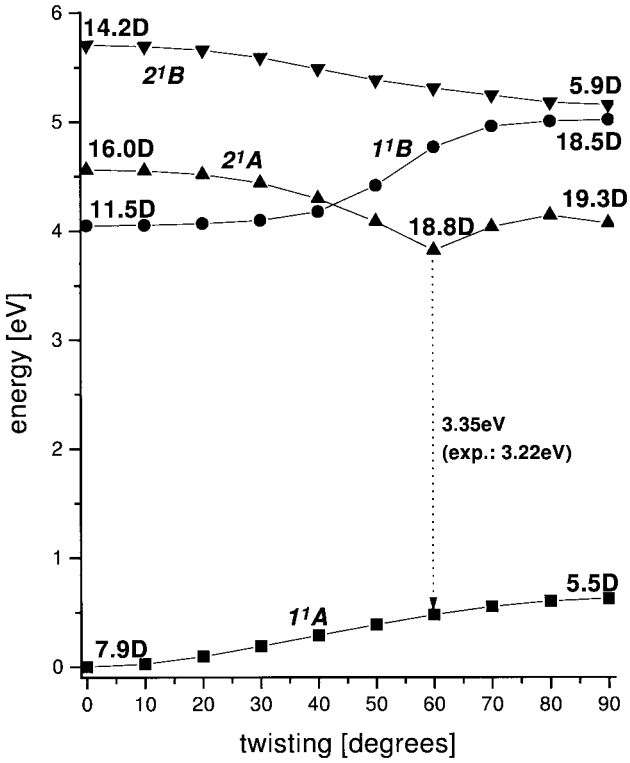

Figure 4. DFT/SCI potential energy curves (energy relative to the C_{2v} minimum of the ground state) of planar DMABN as a function of the dimethylamino twisting angle δ (TICT).

probability and is discussed in detail in section 4. Energetically, the 2A state stabilizes upon rotation and becomes the first excited state for angles δ larger than 40°. At about 60° a minimum is located which is separated from a second local minimum at $\delta = 90°$ by a barrier of approximately 7 kcal/mol (0.3 eV). The planar conformation of the first excited state is stabilized by about 0.5 kcal/mol (0.02 eV) compared to the S_1 perpendicular conformation but 5.2 kcal/mol (0.23 eV) higher in energy than the minimum at 60°. The one-dimensional reaction coordinate without excited-state geometry optimization does not represent the lowest energy path on the multidimensional energy surface. Nevertheless, according to this crude approximation, a barrier of 2.9 kcal/mol (0.13 eV) for the TICT state formation from the 1B state is calculated. The vertical $S_1 \rightarrow S_0$ excitation energy found at $\delta = 60°$, which should be compared with the maximum of the fluorescence band at 3.2 eV, is 3.35 eV.

Experimentally, the DMABN crystal structure[69] as well as the ground-state structure estimated from microwave spectroscopy[70] shows a small pyramidalization angle at the amino group. To take this effect into account, the calculations along the twisting coordinate are repeated with a pyramidalization angle ω of 20°.

The results are presented in Figure 5. The shape of potential energy curves of the three excited states considered is very similar to the nonwagged situation (see Figure 4). The dipole moment of the first excited state rises from 11.2 D ($\delta = 0°$) to 19.3 D at the perpendicular conformation. Due to a complete loss of symmetry, an avoided crossing of the S_1 and S_2 states at about $\delta = 40°$ is now observed. The S_1 is characterized for small twisting angles by an HOMO → LUMO+1 transition (L_b), while for large angles an intramolecular CT state is generated, which is mainly described by a HOMO → LUMO one-electron transition (L_a). Again, a minimum at $\delta = 60°$ is found for the first excited state. The hypothetical barrier between the minima

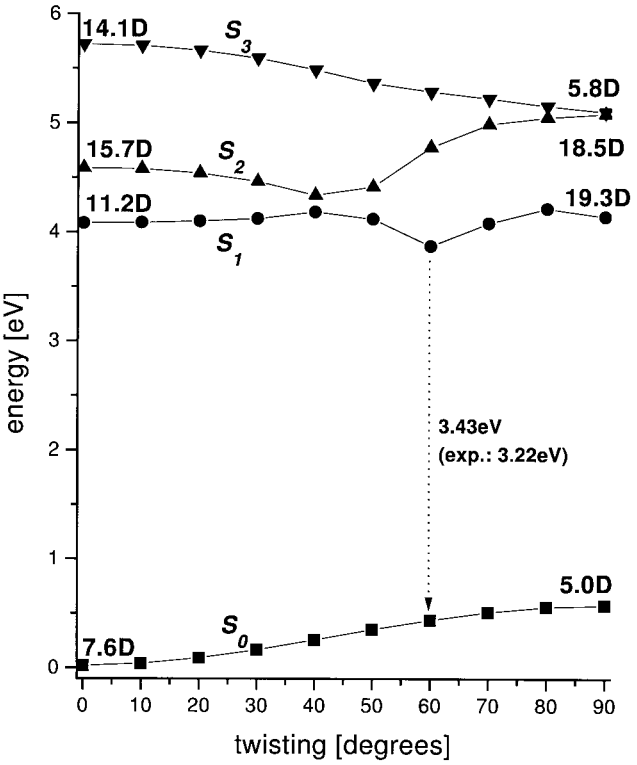

Figure 5. DFT/SCI potential energy curves (energy relative to the C_{2v} minimum of the ground state) of pyramidal ($\omega = 20°$) DMABN as a function of the dimethylamino twisting angle δ (TICT).

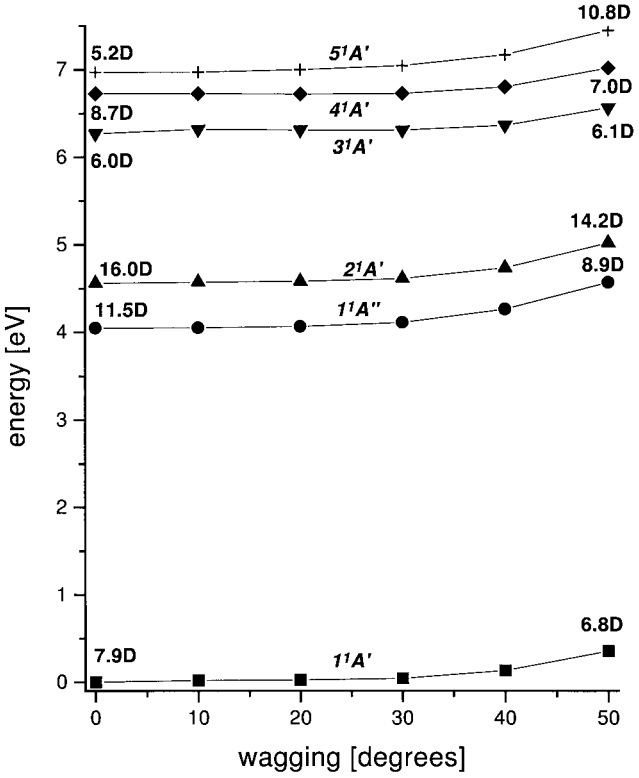

Figure 6. DFT/SCI potential energy curves (energy relative to the C_{2v} minimum of the ground state) for DMABN as a function of the amino group wagging angle ω (WICT).

at $\delta = 0°$ and the transition state at $\approx 40°$ is computed to be 2.3 kcal/mol (0.10 eV), which is only 0.6 kcal/mol lower than in the nonwagged calculation. The vertical emission from the TICT minimum is now calculated to be 3.43 eV. All in all we conclude that the effects of small pyramidalization angles for the three lowest states along the twisting coordinate are insignificant for a discussion of the photophysical behavior of DMABN.

3.3. Potential Curves for the Wagging Mode. Gorse and Pesquer[24] postulated in their work that a pyramidalization of the dimethylamino group is also able to decouple the donor and acceptor subunits so that a highly polar pyramidal (so-called wagged) intramolecular charge transfer (WICT) state is formed.

The results of the calculations along the wagging coordinate ω from a planar system with $\omega = 0°$ to a pyramidal sp^3-hybridized conformation with $\omega = 50°$ are presented in Figure 6. All calculations are carried out in C_s symmetry; thus the former $2A_1$ state is now denoted as $2A'$ and the $1B_2$ state becomes $1A''$. The ground-state potential curve is very flat up to ω values of 30°. As expected, the dipole moment decreases by 1.1 D to $\mu = 6.8$ D at $\omega = 50°$ due to a decreased interaction of the lone pair orbital with the benzonitrile fragment.

The total energies of all low lying excited states increase with increasing pyramidalization, while their dipole moments decrease monotonically as for the ground state. The energy gap between the first and second excited state remains almost unchanged (approximately 0.5 eV), and also for the other excited states no significant changes are found. The lone pair character of the HOMO vanishes along the coordinate, and a π orbital localized in the benzonitrile moiety is generated at large angles. Therefore, the partial CT character for all transitions from the HOMO decreases.

The seventh excited state ($5A'$), with an excitation energy of about 7 eV and a dipole moment of 5.2 D, is characterized by a dominating one-electron transition from the HOMO-2 to the LUMO. The dipole moment of this state increases from 5.2 D ($\omega = 0°$) to 10.8 D ($\omega = 50°$). This transition is characterized by a $n_{sp^3} \rightarrow \pi^*_{benzene}$ excitation leading to an internal CT state, therefore denoted as the WICT state. Nevertheless, no stabilization in energy can be detected for the WICT state, which still remains the S_7 for donor−acceptor decoupled geometries ($\omega = 50°$). The dipole moment of the WICT state (10.8 D) is still smaller than the dipole moments for the first and second excited states at the planar geometry with 11.5 and 16.0 D, respectively.

3.4. Potential Curves for the Rehybridizing Mode. Recently, a new model for the formation of a highly polar CT state in DMABN has been presented by Sobolewski and Domcke.[43,44] According to this model, the CT state is generated by an electron transfer from the dimethylaminobenzene donor to the cyano acceptor group. This state is stabilized by rehybridization from a linear sp to an in-plane bent sp^2 carbon atom of the cyano group (RICT, rehybridization by intramolecular charge transfer). Only the CASPT2 calculations of Sobolewski and Domcke for the RICT pathway have been published so far.

The first and second excited states are of A' symmetry in the C_s point group, which is used throughout these calculations. The fourth excited state, with an excitation energy of 6.27 eV at the planar geometry ($1A_2$ state in C_{2v} symmetry), is characterized (see also section 3.1) as a CT transition from the dimethylanilino donor to the in-plane π^*_x acceptor orbital of the cyano group, with a large dipole moment of 18.1 D. This HOMO $\rightarrow$ LUMO+2 excitation thus represents the RICT state.

Contrary to the situation found along the TICT and WICT pathways, the ground-state energy increases strongly along the RICT coordiante (see Figure 7). The dipole moment decreases significantly to 5.6 D at $\gamma = 110°$. The low-lying $2A'$ and $3A'$ excited states show a similar behavior for the total energy and dipole moment evolution. A large energetic stabilization is seen

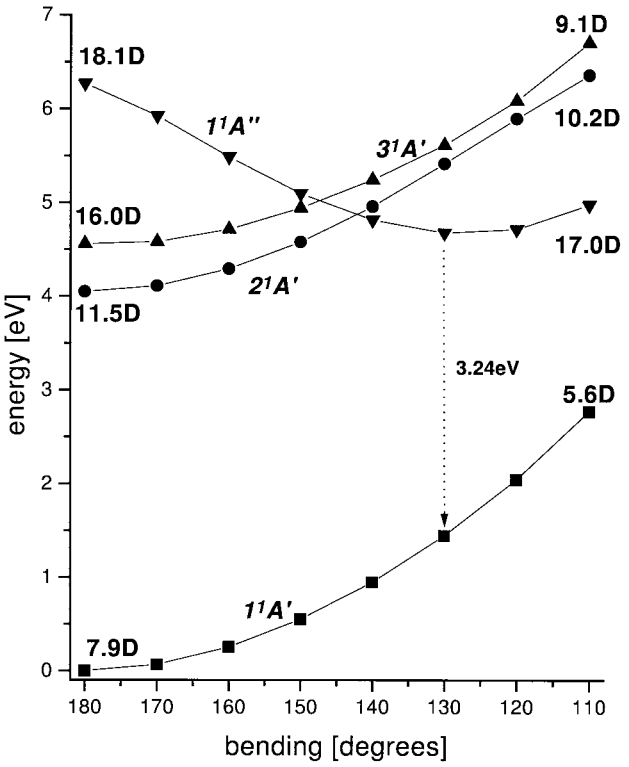

Figure 7. DFT/SCI potential energy curves (energy relative to the C_{2v} minimum of the ground state) for DMABN as a function of the cyano group bending angle γ (RICT).

for the 1A″ state in Figure 7. This state becomes the first excited state for bending angles smaller than 140°, and a minimum in total energy is found at almost complete rehybridization to a sp^2 carbon atom between 130° and 120°. The wave function and dipole moment of the RICT state change very little along the coordinate. At $\gamma = 130°$ a vertical $S_1 \rightarrow S_0$ emission energy of 3.24 eV is calculated. Although this value is quite similar to that obtained in the TICT case, we want to emphasize that the total energy of the RICT minimum is about 0.85 eV higher than the TICT minimum at $\delta = 60°$. The barrier between the planar S_1 geometry and the transition state, i.e., the intersection point of the 2A′ and 1A″ states, is calculated to be 17.6 kcal/mol (0.77 eV).

3.5. Excited States of DMABA and DMABME. The results of the DFT/SCI calculations of the DMABN aldehyde derivative (4-*N*,*N*-dimethylaminobenzaldehyde, DMABA) and the methyl ester derivative (methyl 4-*N*,*N*-dimethylaminobenzoate, DMABME) are summarized together with several experimental data in Table 3. A low lying nπ* transition at 3.93 eV is computed for DMABA. The first excited state of L_b character at 4.04 eV is found only 0.15 eV lower in energy than the L_a state at 4.19 eV.

A similar situation is observed for DMABME. The first excited state of L_b character ($\Delta E = 4.13$ eV) is also quite close to the S_2 state of L_a character ($\Delta E = 4.29$ eV). The nπ* transition for DMABME is calculated at 5.24 eV, strongly blue-shifted in comparison to the aldehyde DMABA.

The energy gap between S_1 and S_2 is thus much smaller for DMABA and DMABME than in DMABN, where an energy difference of 0.51 eV is obtained. Although no inversion of the ordering for the two states is found, we conclude that the S_1 and S_2 states are located at almost the same energy and may couple strongly with each other. The dipole moments for the nπ* states are quite small (DMABA 0.5 D, DMABME 3.0 D), and both L_a and L_b are of highly dipolar character, which is even more significant for the L_a states (DMABA 15.8 D, DMABME 14.9 D).

4. Discussion

The results of the DFT/SCI calculations for planar DMABN are summarized in Table 4 and are compared with experimental and some selected theoretical results. We list here only the 1B and the 2A excited states, which have been investigated in other computations as well.

The absorption spectrum of DMABN in *n*-heptane shows a strong band at 4.4 eV and a weak shoulder at 4.0 eV,[22] difficult to resolve from each other. The electron energy loss spectrum in the gas phase shows an onset at 3.9 eV and a strong signal with a maximum at 4.56 eV, which is not very different from the solution data.[76] There are two main sources for the difference between both numbers. First, there is an uncertainity in electron energy loss experiments (±0.1 eV),[26] and second, different environmental effects yield different energies. The absorption spectrum was obtained in the solvent *n*-heptane, whereas the electron energy loss vertical transition energies result from gas-phase experiments. Our calculations are in excellent agreement with the experimental findings. We therefore attribute the strong signal at 4.4 eV, with an oscillator strength of 0.66 (0.33 according to our measurements[79]), to the allowed $2A_1$ transition having a calculated excitation energy of 4.56 eV. The weak shoulder is assigned to the S_1 state of B_2 symmetry, which is almost forbidden in absorption ($f_{exp} = 0.04$, $f_{calc} = 0.03$). The excitation energy of 4.0 eV agrees very well with our result of 4.05 eV. The dipole moments are systematically too high, i.e., lying 0.5−2 D above the upper limits of the experimental ranges, but changes in the dipole moments and qualitative predictions are quite reliable. The CASPT2 results by Serrano-Andrés et al.[42] and Sobolewski and Domcke[43,44] have the same accuracy, although the $1B_2$ dipole moment, calculated to be 7.6 and 6.9 D, respectively, seems to be underestimated. Concerning the dipole moments, DFT/SCI and CASPT2 are clearly superior to the semiempirical approaches listed, which give essentially no change in dipole moment between the A and B states. The CIS method predicts the excitation energies about 1.0−1.5 eV too high, and the wrong ordering ($2A_1$ below $1B_2$) is found. The L_a and L_b states are known to be separated by more than 0.4 eV from each other. The energy gap $\Delta E(S_2 - S_1)$ is reproduced accurately by DFT/SCI and CASPT2. The CNDO calculations overestimate the energy gap slightly, whereas INDO1 and AM1 underestimate it.

Two distinct emission bands are found in polar solvents; that is, DMABN shows dual fluorescence. Also in the nonpolar cyclohexane solvent a very weak shoulder at 3.2 eV is found besides the strong normal ^1L_b fluorescence at 3.6 eV.[19] The results of our calculations for 90° twisted DMABN along with experimental results are summarized in Table 5. The DFT/SCI data seem to be the best theoretical results available. The fluorescence band energy of 3.35 eV of the intermediate twisted geometry ($\delta = 60°$) is about 0.6 eV lower than the CASPT2 results of Sobolewski and Domcke[42] and yields a better description than all other semiempirical and ab initio results. The experimental fluorescence maximum at 3.2 eV is in good agreement with our result. The dipole moment of the emissive 2A state is determined experimentally to be 14−20 D (see Table 5). The DFT/SCI results of 19.3 D are again at the upper limit of experimental data, in contrast to the CASPT2 dipole moment of 15.6 D.[42]

A discrepancy compared to other computations is found for the evolution of the dipole moment of the 1B state along the

TABLE 3: Comparison of Experimental and Calculated (DFT/SCI(VDZP)) Vertical Excitation Energies (ΔE, in EV) and Dipole Moments (μ, in D) for DMABAc, DMABA, DMABME, DMAEE, and DMABN. The Experimental Data Refer to *n*-Hexane Solution

	DMABAc	DMABA			DMABME			DMABEE	DMABN
	expt[a]	expt[b]	DFT/SCI		expt[c]	DFT/SCI		expt[d]	expt[e]
	ΔE	ΔE	ΔE	μ	ΔE	ΔE	μ	ΔE	ΔE
L_b		4.0	4.04	12.7		4.13	8.2		4.0
L_a	4.1	3.8[f]	4.19	15.8	4.6	4.29	14.9	4.1	4.4
$n\pi^*$		3.5	3.93	0.5		5.24	3.0		

[a] Ref 45. [b] Ref 46. [c] Ref 47. [d] Ref 49. [e] Refs 11, 12, 19, 71−75. [f] $\mu = 14$ D.[83]

TABLE 4: Comparison of Experimental and Theoretical Vertical Excitation Energies (ΔE in eV), Oscillator Strenghts (f), and Dipole Moments (μ in D) of Planar DMABN (C_{2v})

			theoretical method					
		expt[a]	CNDO1[b]	INDO1[c]	AM1/CISD[d]	CIS[e]	CASPT2[f]	DFT/SCI
S_0	μ	5−7			5.6	9.5	7.4	7.9
$2A_1$	ΔE	4.4	4.87	4.63	4.09	5.26	4.41	4.56
	f	0.33	0.242	0.335	0.285	0.638	0.416	0.658
	μ	11−14		8.4	10.7	9.1	13.8	16.0
$1B_2$	ΔE	4.0	4.28	4.40	4.01	5.66	4.05	4.05
	f	0.04	0.019	0.06	0.017	0.058	0.010	0.027
	μ	8−11		9.0	9.4	5.4	7.6	11.5

[a] Refs 11, 12, 19, 71−75, 79. [b] Ref 6. [c] Ref 25. [d] Ref 84. [e] Parusel, A. Unpublished results (3-21+G*). [f] Ref 42.

TABLE 5: Comparison of Experimental and Theoretical Vertical Excitation Energies (ΔE, in eV), Oscillator Strengths (f), and Dipole Moments (μ, in D) of Twisted DMABN (C_{2v})

		expt[a]	CNDO1[b]	INDO1[c]	AM1/CISD[d]	CIS[e]	CASPT2[f]	DFT/SCI[g]
S_0	μ	5−7	0.7		3.6	6.3		5.5
$1A_2$[h]	ΔE	3.2	4.71	4.20	4.92	6.20	3.94	3.44 (3.35)
	f		0.00	0.00	0.000	0.014	0.000	0.000 (0.193)
	μ	14−20		14.0	19.1	14.6	15.6	19.3 (18.8)
$1B_1$[i]	ΔE	3.6	4.48	4.85	4.45	6.19	5.23	4.39 (4.53)
	f		0.013	0.000	0.001	0.188	0.003	0.000 (0.004)
	μ			5.41	4.2	5.4	5.7	18.5 (5.9)

[a] Refs 11, 12, 19, 71−75, 79. [b] Ref 6. [c] Ref 25. [d] Ref 84. [e] Parusel, A. Unpublished results (3-21+G*). [f] Ref 42. [g] The values in parentheses refer to the C_2 minimum at 60° (2A state) and to the 2B state in the 1B state section of the table. [h] $2A_1$ for planar DMABN. [i] $1B_2$ for planar DMABN.

twisting coordinate. In general, a decrease is computed with all other methods, whereas a significant rise up to 18.5 D is found by DFT/SCI. As the 1B state is also of CT character (an excitation from the lone pair at the nitrogen atom to the benzonitrile acceptor subunit is involved), the increase of the dipole moment is explained by the increasing lone pair character of the HOMO orbital upon rotation.

Gedeck and Schneider[37] denote the second state of B symmetry a TICT-2 state. This highly polar state is placed in our calculations very near the 1B state at $\delta = 90°$, whereas semiempirical calculations[37] find it at higher energies (S_4). In their treatment the locally excited 2B state is lowered in energy and becomes the lowest excited state of B symmetry for perpendicular geometry.[37] However, this state crossing is not found in our investigation. The locally excited HOMO-1 → LUMO excitation remains energetically above the 1B CT excited state of HOMO → LUMO+1 character. The dipole moment of 5.9 D ($\delta = 90°$) for the LE state is in good agreement with the theoretical results obtained by the CASPT2 method (5.7 D).[42] In the calculations for the wagged conformation of twisted DMABN ($\delta = 90°$ and $\omega = 20°$) this LE state of B symmetry is located almost at the same energy as the CT state with B symmetry (ΔE(2B − 1B) = 0.02 eV) and can thus account for a small dipole moment of the 1B state at a pyramidal geometry. No explicit experimental data are available concerning the 1B dipole moment.

The excitation energies for the lowest B and A states of the wagged conformation of DMABN are calculated to be very similar to the planar structure, i.e., 4.06 and 4.57 eV, respectively. Our total excited-state energies for the wagged form along the twisting coordinate are essentially the same or lie slightly above the corresponding nonwagged values and therefore support the common picture that the DMABN amino group in its emitting state is planar with a sp^2-hybridized nitrogen.

At first sight it seems quite surprising that the amino group in the emitting TICT state is not fully twisted to 90°. However, also CASPT2 calculations find a flat potential curve for the A state with a shallow minimum at intermediate twisting angles.[42,80] Because the oscillator strength of the A state depends critically on the twisting angle, it seems possible to derive some information about this geometric property from a comparison of theoretical and experimental data. The $f(\delta)$ depdendence of the A state has been investigated by Calzaferri and Rytz[36] employing the extedend Hückel method. They also reached the conclusion that the emitting TICT state cannot be fully twisted, that the TICT emission is z polarized, and that their finding is in agreement with the experimental observations.

In our C_2 calculations the oscillator strength for the A state decreases from 0.66 at $\delta = 0°$ to 0.193 at $\delta = 60°$. At $\delta = 70°$ the transition is already quite weak with $f = 0.08$, and it becomes completely forbidden ($A_1 \rightarrow A_2$) at $\delta = 90°$. Experimentally, the situation is less clear. According to the most reliable data from Schuddeboom et al.,[12] the ratio of the radiative lifetimes of the A(TICT) and B(LE) states is about 0.4 in solvents of low polarity. Thus, if we take $f_{LE} = 0.04$[12,81] we arrive at an estimation of $f = 0.016$ for the emitting TICT

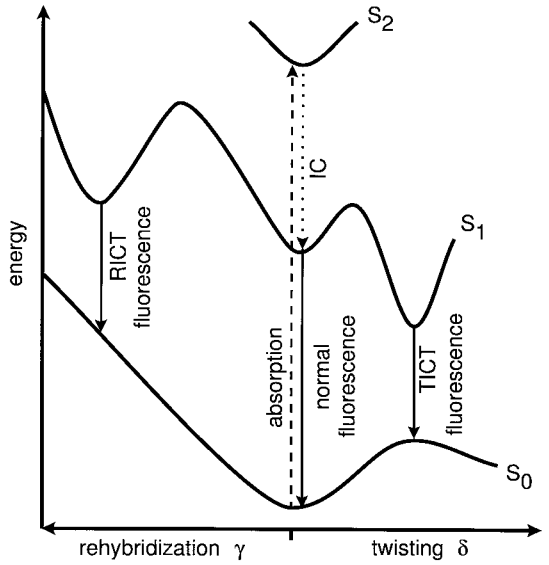

Figure 8. Schematic potential energy curves for the ground and first excited states of DMABN along the twisting and rehybridization coordinate pictured on a two-dimensional hypersurface.

state. This corresponds to a twisting angle of about 80°, i.e., larger than predicted by our DFT/SCI calculations (60°) and by the CASPT2 method (about 45°).[42,80] However, it should be mentioned that the potential surface in this region is very flat and that the dipole moment increases with increasing twisting angle so that even in nonpolar solvents the minimum may be near 90°. However, an f value of 0.016 (which corresponds to ϵ_{max} of about 1000−2000 M^{-1} cm^{-1}) seems to be too high, so that it can be explained to result from an A_2 state by vibronic coupling or intensity borrowing. (The calculated f values change very little in the $\delta = 90°/\omega = 20°$ geometry, i.e., near C_{2v} symmetry is retained for small wagging angles. Intensity borrowing is also very unlikely because the nearest lying state with a significant transition moment (3A at 5.31 eV with $f = 0.435$ in our treatment) is too far away.) Thus, we conclude that the theoretical prediction of an incompletely twisted TICT geometry in the gas phase does not contradict any experimental results and that the geometry of the solvated TICT state seems to have about 80° twist angle.

The results of our calculations are qualitatively summarized in Figure 8. After photoexcitation to the second excited state ($2A_1$), radiationless deactivation to S_1 ($1B_2$) occurs via internal conversion. The system relaxes into the minimum of the planar 1B state, out of which the normal LE fluorescence occurs. The activation barrier for the TICT state formation (about 2.5 kcal/mol) seems to be slightly underestimated because no dual fluorescence in the gas phase is observed (a barrier of 8 ± 0.7 kcal/mol can be estimated in an alkane solvent according to the experimental results of Hicks et al.[82]).

The present theoretical study strongly supports the formation of a twisted intramolecular CT state in DMABN which stabilizes by rotation to an energy somewhat lower than that of the 1B state at nontwisted conformations. A destabilization in energy and decrease in dipole moment of the ground and all excited states is computed along the wagging coordinate, thus disfavoring the wagging motion in general. Only the seventh excited state (5A′) shows an increase in dipole moment (10.8 D at $\omega = 50°$) and some decoupling of the donor from the acceptor group for large wagging angles ω (WICT state). The slight increase of the dipole moment may not be sufficient to stabilize the S_7 state in polar solution below the TICT state because both the S_1 and S_2 dipole moments are even larger at planar geometries.

Zachariasse et al.[19−23] postulate two close lying excited states for DMABN which strongly couple with each other. This small energy gap between the LE and CT states should cause a decoupling of the nitrogen lone pair from the π electrons of the benzonitrile subunit. However, this solvent-induced vibronic decoupling requires a small energy gap, which is not found in our calculations. Independently from the wagging motion, the energy gap between S_1 and S_2 remains almost constant. A value of about 0.5 eV by far exceeds the gap required for an efficient vibronic coupling. Nevertheless, the highly polar S_2 state is stabilized more efficiently in polar solvents than the less polar L_b state ($\Delta\mu = 4.5$ D), which may result in a smaller energy gap in polar solvents. We cannot corroborate the model of Zachariasse et al. by our gas-phase calculations but can also not exclude its importance for solvated DMABN.

Finally we have examined the rehybridizing motion of the cyano group. The former B and A states as well as the ground state show a similar increase in total energy upon bending the cyano group out of the linear arrangement. The promotion of an electron out of the HOMO into the LUMO+2, which is of cyano in-plane π_x^* character, describes the formation of the so-called RICT state. For bending angles smaller than 140° this RICT state becomes the first excited state. Similar to what was found with CASPT2,[43,44] the elongation of the CN bond lengths significantly stabilizes the RICT state along the path. The transition state on the hypersurface from the L_b state toward a stabilized RICT state is calculated to be 17.6 kcal/mol (0.77 eV). The RICT state is 19.6 kcal/mol (0.85 eV) higher in energy than the TICT minimum at $\delta = 60°$. Thus, even in polar solvents the TICT pathway for DMABN is thermodynamically and kinetically favored against the RICT reaction. A similar conclusion concerning the thermodynamic aspect has been obtained only at the CASPT2 level.[44]

The L_a and L_b states of the keto derivatives of DMABN are energetically almost equal. A strong mixing between both states has been observed experimentally, so that these excited states could be assigned only by an analysis of the transition moment directions.[51] The experimental L_a absorption band of DMABN at 4.4 eV shows a strong red-shift for DMABAc (4.1 eV), DMABA (3.8 eV), and DMABEE (4.1 eV). The L_a absorption energy of 4.6 eV for DMABME[47] is not correct in our opinion, because a red-shift is to be expected for DMABME as for all other keto derivatives. A slight blue-shift of the L_b band is obtained in our calculations, but the L_b state still remains located below the L_a. The energy gaps are less than 0.16 eV, in agreement with the experimental observation that the apolar solvent hexane already causes the inversion of L_b and L_a. In our calculations we obtain a significant red-shift for the L_a band of DMABA (4.19 eV) and DMABME (4.29 eV) in comparison to DMABN (4.56 eV), again in agreement with experiment. The small experimental blue-shift for the L_b band of DMABEE[51] of approximately 0.1 eV is also accurately reproduced (0.08 eV). We therefore are able to comprehend the nearly equal L_a and L_b energies caused by a slight L_b blue-shift and a significant L_a red-shift.

The nπ* transition of DMABA is experimentally found to be the first excited state at 3.5 eV and computed at 3.93 eV by DFT/SCI. This quite large error may be traced back to the strong nonvertical nature of this transition (large geometric relaxation in the −CHO group). In DMABEE the nπ* state is experimentally found at higher energies[50] and obtained as the third excited state by our calculations (at 5.24 eV). The DFT/SCI method is capable of giving the correct assignment of the

$n\pi^*$ states as well as a good description of the L_a/L_b state mixing, which is known to be a sensitive test for quantum mechanical methods.

5. Conclusion

In the present work we have studied DMABN and some derivatives with a density functional method including single excitation CI for the description of excited-state properties. The DFT/SCI method has been proven to be a reliable tool for the investigation of excited charge-transfer states. As found previously, the excitation energies obtained by DFT/SCI are in most cases accurate to 0.1−0.2 eV. Comparative calculations on the aldehyde and methyl ester derivative have been carried out as well. Both the L_a and L_b state energies are known to be almost equal in these compounds, a fact that could be corroborated by our method. All in all the DFT/SCI results seem to be of the same accuracy as those obtained by the more elaborate CASPT2 method.

Three different models for the dual emission phenomenon have been considered. First, the TICT model of Grabowski et al.[11,12] which postulates a rotational motion of the dimethylamino group as the excited-state-relaxing motion. Second, the model of decoupling the donor and acceptor subunits by a pyramidalization (wagging) motion at the amino nitrogen, generating the so-called WICT state was investigated. Lastly, the recently published model of a rehybridizing motion of the linear cyano group with an in-plane bent sp^2 carbon atom (RICT) was considered. All models have an intramolecular charge transfer mechanism in common but differ in the relaxation modes. We have been able to show that both the twisting and the rehybridizing pathways yield a minimum on the S_1 energy surface. For DMABN the large energy barrier between the planar S_1 and the RICT state ruled out this pathway as a relaxation mode to explain the dual fluorescence. The small barrier for the TICT state formation accounts for the experimentally observed second emission band. Opposed to what was originally assumed for this state, we find not the fully twisted (perpendicular) structure as the emitting species but a structure with a intermediate twist angle of about 60°. On the other hand, the WICT model could not be corroborated mainly because the polar WICT state is too high in energy and yields furthermore no minimum along the reaction coordinate.

A challanging goal for future studies is the inclusion of solvation effects and the extension to more complex chromophores where additional reaction pathways have to be considered.

Acknowledgment. The authors want to thank Prof. A. L. Sobolewski for helpful discussions and Prof. W. Rettig for help with the derivatives of DMABN. Thanks are also due to Dr. K. Rechthaler for his help with last-minute measurements on DMABN. A.P. and G.K. are indebted to the *Fonds zur Förderung der wissenschaftlichen Forschung* (P 11880-CHE) in Austria for generous financial support.

References and Notes

(1) Lippert, E.; Lüder, W. *Advances in Molecular Spectroscopy*; Mangini, A., Ed.; Pergamon Press: Oxford, 1962.
(2) Platt, J. *J. Chem. Phys.* **1949**, *17*, 484.
(3) Rettig, W. *Angew. Chem., Int. Ed. Engl.* **1986**, *25*, 971.
(4) Rettig, W. *Top. Curr. Chem.* **1994**, *169*, 253.
(5) Rettig, W.; Lapouyade, R. *Topics in Fluorescence Spectroscopy*; Lakowicz, J. R., Ed.; Plenum Press: New York, 1994; Vol. 4.
(6) Khalil, O. S.; Hofeldt, R. H.; McGlynn, S. P. *Chem. Phys. Lett.* **1972**, *17*, 479.
(7) Kosower, E. M.; Dodiuk, H. *J. Am. Chem. Soc.* **1976**, *98*, 924.
(8) Chandross, E. *Exciplex*; Gordon, M., Ware, W. R., Eds.; Academic Press: New York, 1975.
(9) Visser, R. J.; Weisenborn, P. C. M.; Varma, C. A. G. O. *Chem. Phys. Lett.* **1985**, *113*, 330.
(10) Köhler, G.; Grabner, G.; Rotkiewicz, K. *Chem. Phys.* **1993**, *173*, 275.
(11) Rotkiewicz, K.; Grellmann, K. H.; Grabowski, Z. R. *Chem. Phys. Lett.* **1973**, *19*, 315.
(12) Grabowski, Z. R.; Rotkiewicz, K.; Siemiarczuk, A.; Cowley, D. J.; Baumann, W. *Nouv. J. Chim.* **1979**, *3*, 443.
(13) Rotkiewicz, K.; Grabowski, Z.; Krówczyński, A. *J. Lumin.* **1976**, *12−13*, 877.
(14) Rettig, W.; Rotkiewicz, K.; Rubaszewska, W. *Spectrochim. Acta* **1984**, *40A*, 241.
(15) Wermuth, G.; Rettig, W. *J. Phys. Chem.* **1984**, *88*, 2729.
(16) Rettig, W.; Gleiter, R. *J. Phys. Chem.* **1985**, *89*, 4676.
(17) Rotkiewicz, K.; Rubaszewska, W. *Chem. Phys. Lett.* **1980**, *70*, 444.
(18) Rettig, W.; Suppan, P.; Vauthey, E.; Rotkiewicz, K.; Luboradzki, R.; Suwinska, K. *J. Phys. Chem.* **1993**, *97*, 13500.
(19) Gibson, E. M.; Jones, A. C.; Philips, D. *Chem. Phys. Lett.* **1987**, *136*, 454.
(20) Zachariasse, K. A.; von der Haar, T.; Leinhos, U.; Kühnle, W. *J. Inf. Rec. Mater.* **1994**, *21*, 501.
(21) Leinhos, U.; Kühnle, W.; Zachariasse, K. A. *J. Phys. Chem.* **1991**, *95*, 2013.
(22) Zachariasse, K. A.; von der Haar, T.; Hebecker, A.; Leinhos, U.; Kühnle, W. *Pure Appl. Chem.* **1993**, *65*, 1745.
(23) Zachariasse, K. A.; Grobys, M.; Haar, von der T.; Hebecker, A.; Il'ichev, Y.; Morawski, O.; Rückert, I.; Kühnle, W. *J. Photochem. Photobiol. A: Chem.* **1997**, *105*, 373.
(24) Gorse, A.-D.; Persquer, M. *J. Phys. Chem.* **1995**, *99*, 4039.
(25) Lipiński, J.; Chojnacki, H.; Grabowski, Z. R.; Rotkiewicz, K. *Chem. Phys. Lett.* **1980**, *70*, 449.
(26) Rullière, C.; Grabowski, Z. R.; Dobkowski, J. *Chem. Phys. Lett.* **1987**, *137*, 408.
(27) LaFemina, J. P.; Duke, C. B.; Paton, A. *J. Chem. Phys.* **1987**, *87*, 2151.
(28) Rotkiewicz, K.; Leismann, H.; Rettig, W. *J. Photochem. Photobiol. A: Chem.* **1989**, *49*, 347.
(29) Majumdar, D.; Sen, R.; Bhattacharyya, K.; Bhattacharyya, S. P. *J. Phys. Chem.* **1991**, *95*, 4324.
(30) LaFemina, J. P.; Schenter, G. K. *J. Chem. Phys.* **1991**, *94*, 7558.
(31) Bergamasco, S.; Calzaferri, G.; Hädener, K. *J. Photochem. Photobiol. A: Chem.* **1992**, *66*, 327.
(32) Majumdar, D.; Sen, R.; Bhattacharyya, K.; Bhattacharyya, S. P. *J. Photochem. Photobiol. A: Chem.* **1993**, *73*, 177.
(33) Fonseca, T.; Kim, H. J.; Hynes, J. T. *J. Photochem. Photobiol. A: Chem.* **1994**, *82*, 67.
(34) Soujanya, T.; Saroja, G.; Samanta, A. *Chem. Phys. Lett.* **1995**, *236*, 503.
(35) Broo, A.; Zerner, M. C. *Theor. Chim. Acta* **1995**, *90*, 383.
(36) Calzaferri, G.; Rytz, R. *J. Phys. Chem.* **1995**, *99*, 12141.
(37) Gedeck, P.; Schneider, S. *J. Photochem. Photobiol. A: Chem.* **1997**, *105*, 165.
(38) Rettig, W.; Bonačić-Koutecký, V. *Chem. Phys. Lett.* **1979**, *62*, 115.
(39) Kato, S.; Amatatsu, Y. *J. Chem. Phys.* **1990**, *92*, 7241.
(40) Gorse, A.-D.; Pesquer, M. *J. Mol. Struct. (THEOCHEM)* **1993**, *281*, 21.
(41) Hayashi, S.; Ando, K.; Kato, S. *J. Phys. Chem.* **1995**, *99*, 955.
(42) Serrano-Andrés, L.; Merchán, M.; Roos, B. O.; Lindh, R. *J. Am. Chem. Soc.* **1995**, *117*, 3189.
(43) Sobolewski, A. L.; Domcke, W. *Chem. Phys. Lett.* **1996**, *250*, 428.
(44) Sobolewski, A. L.; Domcke, W. *Chem. Phys. Lett.* **1996**, *259*, 119.
(45) Revill, J.; Brown, R. *J. Fluoresc.* **1992**, *2*, 107.
(46) Dobkowski, J.; Kirkor-Kaminska, E.; Koput, J.; Siemiarczuk, A. *J. Lumin.* **1982**, *27*, 339.
(47) Revill, J. Brown, R. *Chem. Phys. Lett.* **1992**, *188*, 433.
(48) Rettig, W.; Wermuth, G.; Lippert, E. *Ber. Bunsen-Ges. Phys. Chem.* **1979**, *83*, 692.
(49) Wermuth, G. *Z. Naturforsch.* **1983**, *38a*, 368.
(50) Wermuth, G.; Rettig, W.; Lippert, E. *Ber. Bunsen-Ges. Phys. Chem.* **1981**, *85*, 64.
(51) Dedonder-Lardeux, C.; Jouvet, C.; Martrenchard, S.; Solgadi, D.; McCombie, J.; Howells, B.; Palmer, T.; Subaric-Leitis, A.; Monte, C.; Rettig, W.; Zimmermann, P. *Chem. Phys.* **1995**, *191*, 271.
(52) Rettig, W.; Dedonder-Lardeaux, C.; Jouvet, C.; Martrenchard-Barra, S.; Szrifiger, P.; Krim, L.; Castano, F. *J. Chim. Phys.* **1995**, *92*, 465.
(53) Roos, B. O.; Fülscher, M.; Malmqvist, P.-A.; Merchan, M.; Serrano-Andrés, L. *Quantum Mechanical Electronic Structure Calculations with Chemical Accuracy*; Langhoff, S. R., Ed.; Kluwer Academic Publishers: Dordrecht, 1995.
(54) Peyerimhoff, S.; Buenker, R. *Excited States in Chemistry*; Nikolaides, C. A., Beck, D. R., Eds.; Reidel: Dordrecht, 1978.

(55) Parr, R. G.; Yang, W. *Density-Functional Theory of Atoms and Molecules*; Oxford University Press: Oxford, 1989.
(56) Grimme, S. *Chem. Phys. Lett.* **1996**, *259*, 128.
(57) Grimme, S.; Pischel, I.; Laufenberg, S.; Vögtle, F. *Chirality* **1998**, *10*, 147.
(58) Engemann, C.; Köhring, G.; Pantelouris, A.; Hormes, J.; Grimme, S.; Peyerimhoff, S. D.; Clade, J.; Frick, F.; Jansen, M. *Chem. Phys.* **1997**, *221*, 189.
(59) Bulliard, C.; Allan, M.; Smith, J. M.; Hrovat, D. A.; Borden, W. T.; Grimme, S. *Chem. Phys.* **1997**, *225*, 153.
(60) Pulm, F.; Schramm, J.; Lagier, H.; Hormes, J.; Grimme, S.; Peyerimhoff, S. D. *Chem. Phys.* **1997**, *224*, 143.
(61) Casida, M. E. *Recent Advances in Density Functional Methods, Vol. 1*; Chong, D. P., Ed.; World Scientific: Singapore, 1995.
(62) Gross, E. K. U.; Dobson, J. F.; Petersilka, M. *Top. Curr. Chem.* **1996**, *181*, 81.
(63) Hashimoto, M.; Hamaguchi, H. *J. Phys. Chem.* **1995**, *99*, 7875.
(64) Ahlrichs, R.; Bär, M.; Häser, M.; Horn, H.; Kölmel, C. *Chem. Phys. Lett.* **1989**, *162*, 165.
(65) Treutler, O.; Ahlrichs, R. *J. Chem. Phys.* **1995**, *102*, 346.
(66) Becke, A. *J. Chem. Phys.* **1993**, *98*, 5648.
(67) Stephens, P. J.; Devlin, F. J.; Chabalowski, C. F.; Frisch, M. J. *J. Phys. Chem.* **1994**, *98*, 11623.
(68) Dunning, T.; Hay, P. *Modern Theoretical Chemistry Vol. 3: Methods of Electronic Structure Theory*; Schaefer, H. F., III, Ed.; Plenum Press: New York, 1977.
(69) Heine, A.; Herbst-Irmer, R.; Stalke, D.; Kühnle, W.; Zachariasse, K. A. *Acta Crystallogr.* **1994**, *B50*, 363.
(70) Kajimoto, O.; Yokoyama, H.; Ooshima, Y.; Endo, Y. *Chem. Phys. Lett.* **1991**, *179*, 455.
(71) Baumann, W. *Z. Naturforsch.* **1981**, *36a*, 868.
(72) Visser, R. J.; Weisenborn, P. C. M.; Varma, C. A. G. O.; DeHaas, M. P.; Warmann, J. M. *Chem. Phys. Lett.* **1984**, *104*, 38.
(73) Weisenborn, P.; Varma, C. A. G. O.; DeHaas, M. P.; Warmann, J. M. *Chem. Phys. Lett.* **1986**, *129*, 562.
(74) Brittinger, C.; Maiti, A.; Baumann, W.; Detzer, N. *Z. Naturforsch.* **1990**, *45a*, 883.
(75) Baumann, W.; Bischof, H.; Frohling, J.; Brittinger, C.; Rettig, W.; Rotkiewicz, K. *J. Photochem. Photobiol. A: Chem.* **1992**, *64*, 49.
(76) Bulliard, C.; Wirtz, G.; Haselbach, E.; Allan, M.; Zacharaisse, K. A.; Detzer, N.; Grimme, S. In preparation.
(77) Marder, S.; Kippelen, B.; Jen, A. K.-Y.; Peyghambarian, N. *Nature* **1997**, *388*, 845.
(78) Schäfer, A.; Horn, H.; Ahlrichs, R. *J. Chem. Phys.* **1992**, *97*, 2571.
(79) Rechthaler, K.; Parusel, A. B. J. Unpublished results.
(80) Sobolewski, A. L.; Sudholt, W.; Domcke, W. *J. Phys. Chem. A* **1998**, *102*, 2716.
(81) Schuddeboom, W.; Jonker, S. A.; Warman, J. M.; Leinhos, U.; Kühnle, W.; Zachariasse, K. A. *J. Phys. Chem.* **1992**, *96*, 10809.
(82) Hicks, J.; Vandersall, M.; Babarogic, Z.; Eisenthal, K. B. *Chem. Phys. Lett.* **1985**, *116*, 18.
(83) Suppan, P. *J. Mol. Spectrosc.* **1969**, *30*, 19.
(84) Gedeck, P. Ph.D Thesis, Universität Nürnberg-Erlangen, 1996.